

Article

# Effect of Annealing Temperature on the Dynamic Characteristics of SS400 Steel Using Experimental Modal Analysis

Andiyanto<sup>1,\*</sup>, Baharudin Priwintoko<sup>1,2</sup>

<sup>1</sup>Department of Mechanical Engineering, Faculty of Engineering, Universitas Diponegoro, Jl. Prof. Soedarto, SH, Tembalang, Semarang 50275, Indonesia

<sup>2</sup>Department of Manufacturing Engineering Technology, Akademi Inovasi Indonesia, Salatiga 50711

\* Corresponding: [andiyanto99@staff.undip.ac.id](mailto:andiyanto99@staff.undip.ac.id)

## ARTICLE INFO

Submitted 19 Oct 2025

Revised 22 Nov 2025

Accepted 7 Dec 2025

Published 31 Dec 2025



The work is licensed under a Creative Commons Attribution-NonCommercial 4.0 International License

## Abstract.

Heat treatment can alter the stiffness-related and energy-dissipation behaviour of structural steels, but its influence on the modal response of SS400 steel is still rarely reported using direct experimental modal testing. This study evaluates the effect of annealing temperature on the dynamic characteristics of SS400 steel specimens under free-free boundary conditions. Four specimen conditions were investigated: raw material and annealed specimens at 700 °C, 800 °C, and 900 °C. Each specimen had dimensions of 200 mm x 20 mm x 5 mm. Experimental modal analysis was conducted using an impact hammer with a fixed uniaxial accelerometer, six roving-hammer measurement points, 10 kHz sampling rate, H1 frequency response function, Hanning windowing, and PolyLSCF stabilization. The first two bending modes were identified. The first natural frequency decreased from 491.655 Hz in the raw material to 434.364 Hz after annealing at 900 °C, corresponding to an 11.65% reduction. The second natural frequency decreased from 1327.165 Hz to 1173.168 Hz, corresponding to an 11.60% reduction. Damping ratios also decreased with increasing annealing temperature, with the largest reduction observed at 900 °C. The results indicate that annealing temperature strongly affects the modal properties of SS400 steel, particularly by reducing frequency- and damping-related indicators at higher temperatures. The contribution of this work is the direct comparison of raw and annealed SS400 modal parameters using the same free-free impact-testing configuration, which provides a baseline modal-response dataset for vibration-sensitive SS400 applications.

**Keywords:** SS400 steel; annealing temperature; experimental modal analysis; natural frequency; damping ratio

## INTRODUCTION

Steel components used in machinery, supporting frames, brackets, fixtures, and structural members are often evaluated primarily through static mechanical properties. However, many engineering failures are also governed

by dynamic response, especially when the component is exposed to cyclic excitation, impact loading, rotating machinery, or resonance-prone operating conditions [1], [2], [3], [4].

SS400 is a widely used low-carbon structural steel because it offers practical weldability, formability, and cost effectiveness for general engineering applications. In manufacturing and repair contexts, thermal exposure or annealing may modify the ferrite-pearlite structure, strength level, hardness, residual-stress state, and stiffness-related response of low-carbon steels [5], [6], [7], [8], [9], [10], [11].

Experimental modal analysis (EMA) provides a direct method for identifying modal parameters from measured input and response signals. In impact-hammer testing, the structure is excited by a measured impulsive force and the response is acquired using vibration transducers, allowing frequency response functions (FRFs), natural frequencies, mode shapes, and damping ratios to be estimated from experimental data [1], [2], [12], [13], [14], [15].

Previous studies show that microstructural variation in steel can influence natural frequency and damping. Heat-treatment studies on carbon and low-carbon steels indicate that changes in grain size, phase distribution, cementite morphology, recovery, recrystallization, and residual stress can alter elastic response, internal friction, and vibration parameters [16], [17], [18].

The specific novelty of this study lies in applying experimental modal analysis directly to SS400 steel specimens subjected to different annealing-temperature conditions and in comparing the resulting natural-frequency, damping-ratio, and normalized dynamic-stiffness trends under the same boundary and measurement configuration. Most related studies discuss heat-treated steels in terms of mechanical or metallurgical properties, whereas the present work emphasizes the modal-response change of SS400 as a structural material.

Therefore, this study aims to evaluate the effect of annealing temperature on the dynamic characteristics of SS400 steel using experimental modal analysis. The investigation focuses on the first two bending modes because these modes are typically the most relevant for low-frequency structural vibration. The specific objectives are: (1) to identify the natural frequency and damping ratio of raw and annealed SS400 specimens, (2) to quantify the percentage changes in modal properties as the annealing temperature increases, and (3) to discuss the implications of the measured trends for vibration-sensitive SS400 components. The study is positioned as an experimental modal-response assessment rather than a complete metallurgical characterization, because the available dataset does not include direct hardness, tensile, density, or metallographic measurements.

## METHODS

### Research design and specimen preparation

This research was designed as an experimental comparison of modal parameters obtained from SS400 steel specimens subjected to different annealing temperature conditions. The specimens consisted of one raw material condition and three annealed conditions: 700 °C, 800 °C, and 900 °C. The specimen dimensions were 200 mm in length, 20 mm in width, and 5 mm in thickness. The test report labels the annealed specimens as having tensile-strength reductions of 30%, 50%, and 60% for the 700 °C, 800 °C, and 900 °C conditions, respectively. Because the present dataset does not include independent tensile-test curves or metallographic images, these labels are treated as specimen-condition descriptors, while the analysis in this manuscript is restricted to the experimental modal parameters. To avoid unsupported mechanical-property claims, the 30%, 50%, and 60% labels are not used as tensile-strength results in the subsequent analysis and are retained only as laboratory specimen identifiers for the three annealing-temperature groups.

The available experimental record confirms the target annealing temperatures of 700 °C, 800 °C, and 900 °C, but it does not provide complete thermal-cycle details such as heating rate, holding time, furnace atmosphere, furnace type, or cooling method. Because these parameters can affect the annealing response, the interpretation is limited to the measured modal-parameter trends, and the absence of complete heat-treatment cycle information is reported as a methodological limitation.

A free-free boundary condition was selected to reduce support-induced stiffness constraints and to approximate the intrinsic bending response of the specimen. The experimental modal analysis was conducted according to the general principles of impact-excitation mobility measurement and modal testing practice [1], [12], [13], [14], [19]. In the test setup, the specimen was suspended using flexible cord-type supports to minimize translational and rotational restraint; the support arrangement was kept the same for all specimen conditions.

The support was intended to provide a low-stiffness suspension relative to the bending stiffness of the steel specimen. Nevertheless, residual support interaction cannot be fully eliminated in a physical free-free modal test; therefore, the reported frequencies and damping ratios should be interpreted as results of the controlled suspended free-free configuration rather than ideal mathematical free-free values.



**Figure 1.** SS400 specimen conditions used in the experimental modal analysis

### **Experimental modal testing configuration**

The modal test used a roving-hammer configuration. The accelerometer was fixed at one response point, while the impact hammer excitation was applied sequentially at six measurement points along the specimen. The measurement direction was the Z+ axis. The excitation device was an impact hammer with a sensitivity of 1.0784 mV/N. The response transducer was a Dytran 355D1T IEPE uniaxial acceleration sensor with a sensitivity of 50.3 mV/g and a frequency response of 1 to 10000 Hz. The data acquisition system was a DE-944 unit connected to Dynatronic modal analysis software. The accelerometer position was maintained constant throughout all tests so that any transducer-related effect remained consistent across specimen conditions.

The exact accelerometer mass was not stated in the available test log. Because the specimen dimensions were relatively small, accelerometer mass loading could slightly reduce the measured natural frequencies, particularly for higher modes. No mass-loading correction was applied in this preliminary dataset; however, the same uniaxial accelerometer and fixed response location were used for all specimens, so the relative comparison among annealing conditions remains internally consistent.

The measured force and acceleration signals were processed using the H1 FRF estimator. Hanning windowing was applied to minimize leakage effects, and PolyLSCF stabilization was used for modal parameter extraction, following common frequency-domain modal-identification practice [15], [20], [21], [22]. Stable poles were selected by considering the consistency of FRF peaks, the PolyLSCF stabilization output, and the physical plausibility of the identified bending-mode shapes.

The dataset did not include numerical coherence values, complete averaged-FRF statistics, MAC matrices, or uncertainty intervals for all tested conditions. Therefore, this manuscript reports deterministic modal parameters and qualitative mode-shape consistency, while the absence of quantitative validation metrics is explicitly acknowledged as a limitation.



**Figure 2.** Experimental modal analysis setup with impact hammer, accelerometer, data acquisition system, and modal analysis software

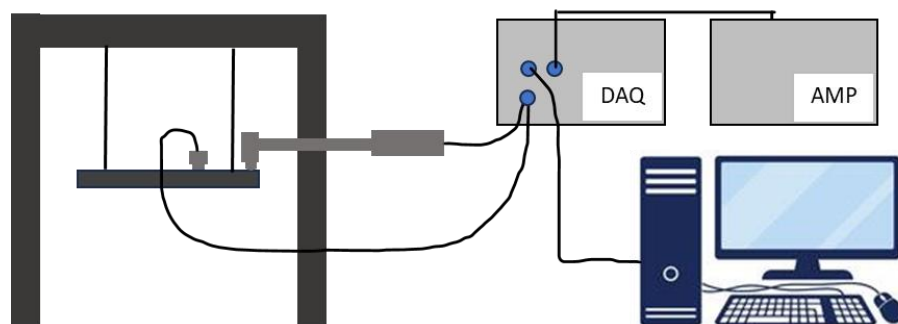


**Figure 3.** Schematic representation of the experimental modal testing system

**Table 1.** Experimental configuration used for SS400 modal testing

Parameter	Specification
Material	SS400 steel
Specimen dimensions	200 mm x 20 mm x 5 mm
Boundary condition	Free-free condition
Excitation method	Impact hammer, roving-hammer method
Number of measurement points	6 points
Accelerometer position	Fixed at one response point
Measurement direction	Z+ axis
Sampling rate	10 kHz
FRF estimator	H1
Windowing	Hanning
Stabilization method	PolyLSCF

Support arrangement	Suspended free-free configuration using flexible cord-type supports; support arrangement kept constant for all specimen conditions
Specimen-level replication	Not available in the supplied dataset; results are reported as deterministic measured values
Modal validation basis	PolyLSCF stabilization, FRF peak consistency, and qualitative bending-mode shape consistency; numerical coherence and MAC values were not available for complete reporting

**Table 2.** Instruments and software used in the modal testing

Equipment	Model	Specification
Exciter	Impact hammer	Sensitivity 1.0784 mV/N
Transducer	IEPE acceleration sensor Dytran 355D1T	Sensitivity 50.3 mV/g; frequency response 1 to 10000 Hz; uniaxial Accelerometer mass was not available in the test log; possible mass-loading effects are discussed as a limitation.
Data acquisition	DE-944	8 channels; ICP transducer support; BNC signal adaptor; 4-20 mA current signal; transient or triggered continuous sampling mode; sweep rate $\leq 1$ octave/min; driving amplitude peak 0.19 mm
Modal software	Dynatronic Software	FRF, multichannel FFT analysis, ICP/IEPE accelerometer support, MAC

### Data processing and derived indicators

The principal output parameters were natural frequency, damping ratio, and mode shape. These modal parameters are commonly used to characterize structural dynamics and to compare experimentally identified dynamic behaviour under different material or boundary-condition states [23], [24].

$$H1(\omega) = G_{yx}(\omega) / G_{xx}(\omega) \quad (1)$$

The percentage change of each parameter relative to the raw material condition was calculated using Equation (2).

$$\Delta P_i (\%) = ((P_i - P_{raw}) / P_{raw}) \times 100\% \quad (2)$$

A relative dynamic stiffness indicator was calculated from the square of the natural-frequency ratio, as shown in Equation (3). This indicator was used only as a comparative index because specimen mass and geometry were assumed constant, while direct modulus measurement was not included in the supplied dataset [17]. Accordingly,  $K_{rel,i}$  is a normalized frequency-squared indicator and should not be interpreted as a direct measurement of elastic modulus or absolute structural stiffness unless mass distribution, support conditions, and measurement configuration are strictly controlled.

$$K_{rel,i} = (f_i / f_{raw})^2 \quad (3)$$

In Equations (2) and (3),  $P_i$  is the measured parameter for an annealed condition,  $P_{raw}$  is the corresponding parameter for the raw material,  $f_i$  is the natural frequency of a given annealed specimen, and  $f_{raw}$  is the natural frequency of the raw material for the same mode.

## RESULT AND DISCUSSION

### Identified modal parameters

The first two modes were consistently identified for all specimen conditions. Table 3 summarizes the measured natural frequencies, damping ratios, mode types, and qualitative descriptions. The raw SS400 specimen showed a first natural frequency of 491.655 Hz and a second natural frequency of 1327.165 Hz. After annealing, both natural frequencies decreased, with the greatest reduction occurring at 900 °C. Because specimen-level replicates and standard deviations were not available, the values in Table 3 are presented as measured modal parameters for the tested specimens rather than statistically averaged population estimates.

**Table 3.** Measured modal parameters of raw and annealed SS400 specimens

Specimen condition	Mode	Natural frequency (Hz)	Damping ratio (%)	Mode type	Description
Raw material	1	491.655	0.296	Bending	One curvature / 1 antinode
Raw material	2	1327.165	0.279	Double bending	Two curvatures / 2 antinodes
Annealed 700 °C	1	489.707	0.255	Bending	One curvature / 1 antinode
Annealed 700 °C	2	1312.053	0.269	Double bending	Two curvatures / 2 antinodes
Annealed 800 °C	1	468.055	0.159	Bending	One curvature / 1 antinode
Annealed 800 °C	2	1265.557	0.178	Double bending	Two curvatures / 2 antinodes

Annealed 900 °C	1	434.364	0.082	Bending	One curvature / 1 antinode
Annealed 900 °C	2	1173.168	0.132	Double bending	Two curvatures / 2 antinodes

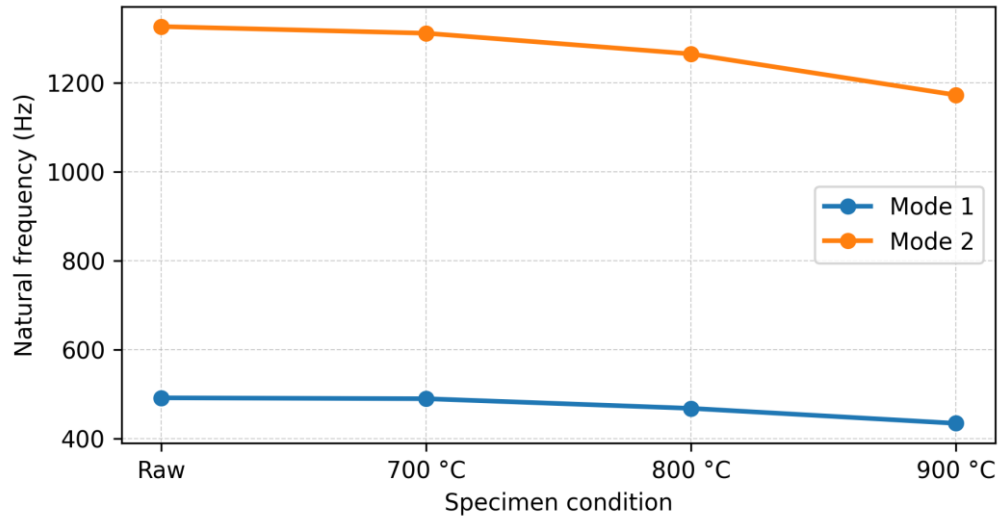


**Figure 4.** Natural-frequency trends of the first two bending modes as a function of specimen condition. Updated plot includes explicit axes, units, and legend for readability

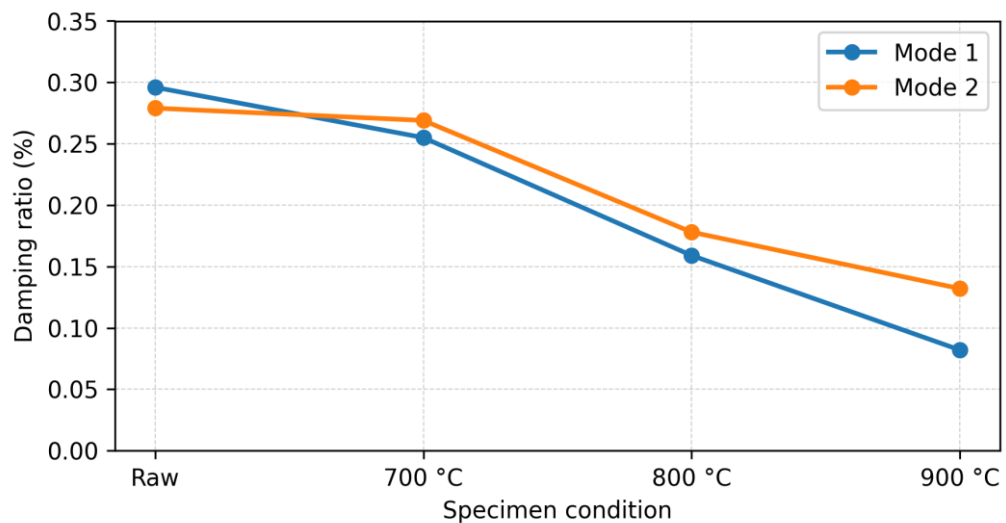


**Figure 5.** Damping-ratio trends of the first two bending modes as a function of specimen condition. Updated plot includes explicit axes, units, and legend for readability

### Effect of annealing temperature on natural frequency

The natural frequency decreased as the annealing temperature increased. In vibration theory, natural frequency is governed primarily by the relationship between stiffness and mass; therefore, for specimens with comparable dimensions and mass, a downward frequency shift can be interpreted as a reduction in stiffness-related dynamic response [3], [4], [19]. This

interpretation assumes unchanged nominal geometry and comparable test configuration; therefore, it describes a measured dynamic-response shift, not an independently verified modulus reduction.

A similar trend was observed for the second bending mode. The second natural frequency decreased from 1327.165 Hz in the raw material to 1312.053 Hz after annealing at 700 °C, 1265.557 Hz after annealing at 800 °C, and 1173.168 Hz after annealing at 900 °C. The corresponding frequency reductions were -1.14%, -4.64%, and -11.60%, respectively. The close similarity between the first-mode and second-mode reductions at 900 °C suggests that the thermal treatment affected the global dynamic stiffness of the specimen rather than only one localized mode.

The ratio of the second natural frequency to the first natural frequency remained relatively stable, ranging from 2.679 to 2.704. This stability supports the observation that the specimens maintained a comparable bending-mode sequence across the investigated annealing temperatures. In a simplified beam-like structure with unchanged geometry and mass distribution, a decrease in natural frequency is commonly associated with a reduction in effective stiffness or elastic-modulus-related response [14], [25]. However, because no direct modulus, density, hardness, or microstructure measurements were included in the dataset, the present interpretation should be treated as a modal-response interpretation rather than a complete metallurgical explanation. The conclusion regarding global stiffness-related response is therefore expressed cautiously and should be confirmed in future work using density, elastic modulus, hardness, and metallographic measurements.

**Table 4.** Percentage changes and derived dynamic indicators relative to raw SS400

Condition	$\Delta f_1$ (%)	$\Delta f_2$ (%)	$\Delta \zeta_1$ (%)	$\Delta \zeta_2$ (%)	Krel mode 1	Krel mode 2	f2/f1
Raw material	0.00	0.00	0.00	0.00	1.000	1.000	2.699
Annealed 700 °C	-0.40	-1.14	-13.85	-3.58	0.992	0.977	2.679
Annealed 800 °C	-4.80	-4.64	-46.28	-36.20	0.906	0.909	2.704
Annealed 900 °C	-11.65	-11.60	-72.30	-52.69	0.781	0.781	2.701

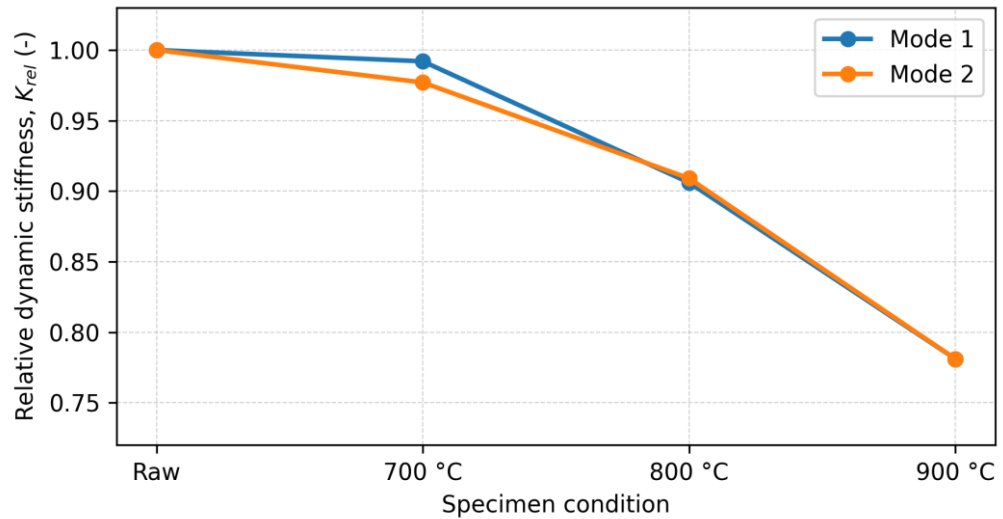


**Figure 6.** Relative dynamic stiffness indicators calculated from the measured natural frequencies. Updated plot includes explicit axes, dimensionless  $K_{rel}$  notation, and legend for readability

### Effect of annealing temperature on damping ratio

The damping ratios also showed a decreasing trend with increasing annealing temperature. Damping in metallic materials is generally sensitive to internal friction, dislocation density, phase interfaces, grain-boundary behaviour, residual stress, and microstructural morphology, which may be modified by heat treatment [26]. In the absence of direct microstructural characterization, these mechanisms are discussed only as possible contributors to the observed damping trend.

The damping response is often more sensitive to microstructural and contact-related energy dissipation mechanisms than natural frequency. Literature on heat-treated metals indicates that damping can either increase or decrease depending on phase distribution, dislocation density, internal friction mechanisms, precipitates, grain size, and residual stress state [7], [8], [9], [10], [11], [27]. Therefore, the decreasing damping ratio observed in this dataset should not be generalized to all annealed steels. Instead, it should be interpreted as the response of the tested SS400 specimens under the given annealing conditions and modal-test configuration. Thus, the modal data support the existence of a treatment-dependent damping change, but they do not by themselves identify the dominant metallurgical mechanism.

The largest damping reduction was recorded at 900 °C. Combined with the approximately 11.6% reduction in natural frequency, this condition represents the most substantial change in dynamic characteristics among the investigated treatments. From a design perspective, a simultaneous decrease in natural frequency and damping ratio can be important because it may shift the component closer to operating excitation frequencies while also reducing the ability of the component to dissipate vibrational energy.

### **Mode-shape interpretation**

The mode-shape classification remained consistent in all tested specimens. The first mode was identified as a bending mode with one antinode, while the second mode was identified as a double-bending mode with two antinodes, which is consistent with the expected response of slender beam-like specimens under free-free modal testing [4].

Although the supplied dataset includes mode-shape and FRF images for each specimen, this manuscript focuses on the numerical modal parameters and overall trends. For a more complete modal validation, future work should report coherence, repeated impacts, averaged FRFs, modal assurance criterion values, and uncertainty intervals [21], [22]. These additions would improve confidence in the extracted modal parameters and allow statistical comparison between thermal treatments. In this revision, the modal validation is therefore described as qualitative, based on stable mode order and consistent bending-mode classification, rather than as a full quantitative validation using coherence or MAC thresholds.

### **Engineering implications and limitations**

The results show that annealing temperature has a measurable influence on SS400 modal behaviour. For components made of SS400 steel, the reduction in natural frequency after higher-temperature annealing may influence resonance margins, particularly when the component operates close to excitation frequencies generated by rotating machinery, impact events, or structural vibration sources [28].

Several limitations should be noted. First, the dataset does not indicate replicate specimens or repeated statistical trials for each annealing condition; therefore, the article does not present inferential statistics. Second, mass, hardness, tensile-test data, and metallographic evidence were not available for independent correlation with the modal trends. Third, only the first two bending modes were considered. These limitations do not invalidate the measured modal trends, but they define the scope of interpretation and suggest that future studies should combine EMA with mechanical testing, metallography, and uncertainty-based modal parameter estimation [17], [18], [26].

Additional limitations are related to the completeness of the experimental record. The heating rate, holding time, furnace atmosphere, cooling method, accelerometer mass, coherence curves, averaged-FRF variability, and MAC values were not available for complete reporting. These missing parameters limit the ability to separate true material effects from possible thermal-cycle, sensor-mass, and modal-identification uncertainties. Future studies should include controlled annealing-cycle documentation, repeated specimens for each condition, repeated impacts with averaged FRFs and coherence reporting, accelerometer mass-loading assessment, and direct mechanical and microstructural characterization.

## CONCLUSION

This study evaluated the effect of annealing temperature on the dynamic characteristics of SS400 steel using experimental modal analysis under free-free boundary conditions. Based on the measured modal parameters, the following conclusions can be drawn.

First, annealing temperature reduced the natural frequency of SS400 specimens. The first natural frequency decreased from 491.655 Hz in the raw material to 434.364 Hz at 900 °C, while the second natural frequency decreased from 1327.165 Hz to 1173.168 Hz. These changes correspond to reductions of 11.65% and 11.60%, respectively. Second, the damping ratio decreased as the annealing temperature increased. The largest damping reduction occurred at 900 °C, where the damping ratio decreased by 72.30% for the first mode and 52.69% for the second mode relative to the raw material. Third, the mode sequence remained consistent across all specimen conditions. The first mode was identified as a bending mode with one antinode, and the second mode was identified as a double-bending mode with two antinodes. This consistency indicates that annealing affected modal parameter values without changing the basic bending-mode classification. Fourth, the relative dynamic stiffness indicator calculated from the natural-frequency ratio decreased to approximately 0.78 at 900 °C for both modes. This suggests a substantial reduction in stiffness-related dynamic response, although direct elastic modulus measurement is required to confirm the material-level mechanism.

Overall, the results demonstrate that experimental modal analysis is a useful non-destructive method for detecting changes in the dynamic behaviour of annealed SS400 steel. Future work should include repeated specimens, tensile testing, hardness measurement, microstructural characterization, and uncertainty analysis to establish a stronger relationship between annealing temperature, mechanical properties, and modal response. The conclusions should therefore be understood as valid for the tested specimens and measurement configuration, while broader generalization requires the additional validation steps described above.

## Acknowledgements

The authors acknowledge the Laboratory of Vibration and Machine Diagnosis, Department of Mechanical Engineering, Faculty of Engineering, Universitas Diponegoro, for providing the experimental modal analysis data and testing facilities. The authors also acknowledge the technical support of the laboratory operator during impact-hammer testing and data acquisition.

## REFERENCES

- [1] D. J. Ewins, *Modal Testing: Theory, Practice and Application*, 2nd ed. Baldock, UK: Research Studies Press, 2000.
- [2] J. He and Z.-F. Fu, *Modal Analysis*. Oxford, UK: Butterworth-Heinemann, 2001.
- [3] D. J. Inman, *Engineering Vibration*, 4th ed. Upper Saddle River, NJ, USA: Pearson, 2014.
- [4] S. S. Rao, *Mechanical Vibrations*, 6th ed. Upper Saddle River, NJ, USA: Pearson, 2017.
- [5] Alfirano, S. Wibawa, and M. Hidayat, "Effect of Intercritical Annealing Temperature and Holding Time on Microstructure and Mechanical Properties of Dual Phase Low Carbon Steel," *Appl. Mech. Mater.*, vol. 493, pp. 721–726, 2014, doi: 10.4028/www.scientific.net/AMM.493.721.
- [6] J. Ayres, D. Penney, P. Evans, and R. Underhill, "Effect of Intercritical Annealing on the Mechanical Properties of Dual-Phase Steel," *Ironmak. & Steelmak.*, vol. 49, no. 8, pp. 821–827, 2022, doi: 10.1080/03019233.2022.2062163.
- [7] Q. Yuan et al., "Rapid Annealing of an Ultralow Carbon Steel: In-Depth Exploration of the Microstructure--Mechanical Properties Evolution," *J. Mater. Res. Technol.*, vol. 27, pp. 1097–1113, 2023, doi: 10.1016/j.jmrt.2023.09.286.
- [8] S. Dewangan, V. V. Nemade, K. H. Nemade, P. M. Bohra, S. R. Kartha, and M. K. Chowrasia, "A Discussion on Mechanical Behaviour of Heat-Treated Low Carbon Steel," *Mater. Today Proc.*, vol. 63, pp. 362–367, 2022, doi: 10.1016/j.matpr.2022.03.203.
- [9] J. Adamczyk and A. Grajcar, "Heat Treatment and Mechanical Properties of Low-Carbon Steel with Dual-Phase Microstructure," *J. Achiev. Mater. Manuf. Eng.*, vol. 22, no. 1, pp. 13–20, 2007.
- [10] H. Dannoshita, T. Ogawa, K. Maruoka, and K. Ushioda, "Effect of Initial Microstructures on Austenite Formation Behavior during Intercritical Annealing in Low-Carbon Steel," *Mater. Trans.*, vol. 60, no. 1, pp. 165–168, 2019, doi: 10.2320/matertrans.M2018298.
- [11] A. Çalik, "Effect of Cooling Rate on Hardness and Microstructure of {AISI} 1020, {AISI} 1040 and {AISI} 1060 Steels," *Int. J. Phys. Sci.*, vol. 4, no. 9, pp. 514–518, 2009.
- [12] "ISO 7626-5:2019: Mechanical Vibration and Shock --- Experimental Determination of Mechanical Mobility --- Part 5: Measurements Using Impact Excitation with an Exciter Which Is Not Attached to the Structure," no. ISO 7626-5:2019. ISO, Geneva, Switzerland, 2019.
- [13] P. Avitabile, *Modal Testing: A Practitioner's Guide*. Hoboken, NJ, USA: John Wiley & Sons, 2017. doi: 10.1002/9781119222989.
- [14] N. M. M. Maia and J. M. M. Silva, *Theoretical and Experimental Modal Analysis*. Taunton, UK: Research Studies Press, 1997.
- [15] J. S. Bendat and A. G. Piersol, *Random Data: Analysis and Measurement Procedures*, 4th ed. Hoboken, NJ, USA: John Wiley & Sons, 2010.
- [16] G. E. Totten, Ed., *Steel Heat Treatment: Metallurgy and Technologies*, 2nd ed. Boca Raton, FL, USA: CRC Press, 2006. doi: 10.1201/9780849384523.
- [17] W. D. Callister Jr. and D. G. Rethwisch, *Materials Science and Engineering: An Introduction*, 10th ed. Hoboken, NJ, USA: John Wiley & Sons, 2018.

- [18] “JIS G 3101:2024: Rolled Steels for General Structure,” no. JIS G 3101:2024. Japanese Standards Association, Tokyo, Japan, 2024.
- [19] J. Campbell, *Complete Casting Handbook: Metal Casting Processes, Metallurgy, Techniques and Design*, 2nd ed. Oxford, UK: Butterworth-Heinemann, 2015.
- [20] P. Guillaume, P. Verboven, S. Vanlanduit, H. der Auweraer, and B. Peeters, “A Poly-Reference Implementation of the Least-Squares Complex Frequency-Domain Estimator,” in *Proceedings of the 21st International Modal Analysis Conference (IMAC XXI)*, Kissimmee, FL, USA, 2003, pp. 183–192.
- [21] B. Peeters, H. der Auweraer, P. Guillaume, and J. Leuridan, “The PolyMAX Frequency-Domain Method: A New Standard for Modal Parameter Estimation?,” *Shock Vib.*, vol. 11, no. 3--4, pp. 395–409, 2004, doi: 10.1155/2004/523692.
- [22] M. T. Steffensen, M. Döhler, D. Tcherniak, and J. J. Thomsen, “Variance Estimation of Modal Parameters from the Poly-Reference Least-Squares Complex Frequency-Domain Algorithm,” *Mech. Syst. Signal Process.*, vol. 223, p. 111905, 2025, doi: 10.1016/j.ymsp.2024.111905.
- [23] R. J. Allemang, “The Modal Assurance Criterion: Twenty Years of Use and Abuse,” *Sound & Vib.*, vol. 37, no. 8, pp. 14–23, 2003.
- [24] M. Pastor, M. Binda, and T. Harcarik, “Modal Assurance Criterion,” *Procedia Eng.*, vol. 48, pp. 543–548, 2012, doi: 10.1016/j.proeng.2012.09.551.
- [25] H. K. D. H. Bhadeshia and R. W. K. Honeycombe, *Steels: Microstructure and Properties*, 4th ed. Oxford, UK: Butterworth-Heinemann, 2017.
- [26] J. L. Dossett and G. E. Totten, Eds., *{ASM} Handbook, Volume 4A: Steel Heat Treating Fundamentals and Processes*. Materials Park, OH, USA: ASM International, 2013. doi: 10.31399/asm.hb.v04a.9781627081658.
- [27] C. Ekinici, N. Ucar, A. Calik, S. Karakas, and I. Akkurt, “Effects of Heat Treatment on the Microstructure and Mechanical Properties of Low-Carbon Microalloyed Steels,” *High Temp. Mater. Process.*, vol. 30, no. 1--2, pp. 39–42, 2011, doi: 10.1515/htmp.2011.005.
- [28] N. M. Yazdani, “Experimental Evaluation of the Effects of Structural Changes on the Vibration Properties of {CK35} Steel,” *Acta Mech. Autom.*, vol. 15, no. 2, pp. 53–57, 2021, doi: 10.2478/ama-2021-0008.